Jet Fluctuations and Drop Velocity Jitter: Confirmation of a Causal Model

Jeremy Grace, Semrock, Inc; Rochester, NY /USA, Carolyn Ellinger, Giuseppe Farruggia, Yonglin Xie; Eastman Kodak Company; Rochester, NY /USA

Abstract

In continuous inkjet devices, an applied perturbation, such as acoustic vibration or thermal modulation, is used to drive the Rayleigh-Plateau instability to cause regular breakup of liquid microjets into droplets of controlled size. Background fluctuations and other processes contribute to subtle variations in droplet velocity within the droplet stream. These velocity variations—droplet velocity jitter—can be observed by stroboscopy or by laser detection. The fluctuations in droplet position or period are influenced by the details of the jet breakup process, and measurement of the droplet fluctuations as a function of distance along the droplet stream provide estimates of the fundamental noise on the jet.

Introduction

Droplet velocity noise is of practical importance in thermally stimulated continuous inkjet technology, wherein thousands of continuous streams of droplets are generated continuously by thermally stimulated jet break-up. In practice, print drops and catch drops are produced, with the former being directed to paper to generate a printed image, while the latter are directed towards a gutter, collected and recirculated. Current Kodak Stream technology employs a large drop print mode wherein the smaller catch drops are separated from the larger print drops by differential deflection in a cross flow of air. Small-drop velocity fluctuations are kept sufficiently small that consecutive catch drops do not merge prior to their arrival to the deflection zone, ensuring that there is sufficient mass differentiation for deflection.

Fluctuations on a Jet

In order to understand droplet velocity jitter, it is helpful to start with the fundamentals of droplet generation. The approach we use here is based on the condition for jet break-up driven by the Rayleigh-Plateau instability with the retarding effect of surface tension on the average velocity of droplets generated from jet break-up. Generation of drops of fluid via jet breakup can be controlled by low-energy pulses applied periodically to a heater situated around a jet orifice [1]. These heating pulses cause changes in the temperature of the fluid and its associated properties and can be considered as mathematically equivalent to applying a radial perturbation to the jet. One can reason that at the time of jet break-up t_b, the perturbation amplitude ξ has grown (at growth rate α) from its initial value ξ_i to equal the jet radius R causing the droplets to separate from the stream: [1, 2]

$$t_b = \frac{1}{\alpha}\ln\left(\frac{R}{\xi_i}\right) \tag{1}$$

The growth rate α depends on the properties of the fluid (i.e., surface tension, viscosity and density), the jet radius, and the frequency of stimulation. Successive break-up events convert the mass flow of the fluid column to a mass flow of droplets. On average, the momentum of the jet must equal the momentum of the stream of droplets after break-up, and the average droplet velocity (v_{drop}) is thus related to the average jet velocity (v_{jet}) by [3]:

$$v_{drop} = v_{jet} - \frac{\sigma}{\rho \cdot v_{jet} \cdot R} \tag{2}$$

Here, σ is the dynamic surface tension (i.e. surface tension on a time scale of the order of the jet break-up time) and ρ is the mass density of the fluid. The column of fluid jetted from the nozzle has a momentum per unit length dictated by the jet velocity, the jet radius, and the density. Any portion of this stream that is partitioned into a droplet acquires the droplet velocity of Equation 2, regardless of size. In the laboratory, this point can be appreciated by generating droplets of vastly different sizes by changing the frequency of heat pulses applied and maintaining a constant energy per droplet. Thus, while the time between break-up events determines the mass of the droplet formed it should have no effect on the droplet velocity. In contrast, fluctuations in the jet velocity will naturally translate to fluctuations in the droplet velocity as can be appreciated by examination of Equation 2.

Fluctuations in the break-up time arising from fluctuations in effective stimulation (Equation 1) are also expected to alter the droplet velocity. The effect of a fluctuating jet velocity can be found by differentiation of Equation 2 to find the relative velocity fluctuation (i.e., $\delta v/v$) for droplets as a function of the relative velocity fluctuation for the jet:

$$\frac{\delta v_{drop}}{v_{drop}} = \left(\frac{1+\dfrac{\sigma}{R\rho v_{jet}^2}}{1-\dfrac{\sigma}{R\rho v_{jet}^2}}\right)\frac{\delta v_{jet}}{v_{jet}} \tag{3}$$

Equation 1, with a growth rate α appropriate for the fluid properties, geometry, and stimulation frequency does an excellent job of predicting break-up times for flows characterized by low Weber number, despite the departure from simple linear behavior near jet break-up, where the perturbation has grown to dominate the jet geometry. In this break-up regime, hereafter called the "pinch-off region", the fluid volume that couples the emerging droplet to the jet becomes vanishingly small. Fluctuations in fluid properties in this regime could have significant impact on the droplet velocity. For example, a fluctuating surface tension would produce a fluctuating droplet velocity in accordance with Equation 2. Furthermore, fluctuations in surface tension and viscosity could produce variations in recoil effects not accounted for in Equation 2, and formation of the droplet and the receding filament may be characterized by fluctuations in droplet size and velocity and filament size and recoil momentum.

In the next section we derive relationships between the experimentally observed fluctuating quantities and the fluctuating quantities in the jet and droplet stream. We will make use of the relationships expressed in Equations. 4 – 7 below. As break-up length (L) is more readily measured than break-up time, it is helpful to make use of the fact that they are related through the jet velocity:

$$t_b = \frac{L}{v_{jet}} \tag{4}$$

Fluctuations in break-up time can thus be related to fluctuations in break-up length and jet velocity:

$$\delta t_b = \frac{\delta L}{v_{jet}} \frac{-L\delta v_{jet}}{v_{jet}^2} \tag{5}$$

Furthermore, differentiating Equation 2 yields:

$$\delta t_b = \frac{-1}{\alpha}\left(\frac{\delta\xi_i}{\xi_i}\right) \equiv \delta t_j \tag{6}$$

Hence, fluctuations in break-up length and jet velocity can be related to the fluctuations in radial perturbation, which are believed to arise from boundary layer fluctuations in the nozzle.

Finally, as we have argued that there is likely a significant contribution to drop velocity fluctuations that has its origins at jet break-up in the pinch-off region (and not in the nozzle); we introduce a separate fluctuation in break-up time from this cause. We make a distinction between variation in break-up time δt_j from fluctuations on the jet as it emerges from the nozzle and a variation in break-up time δt_p from fluctuations in the pinch-off region:

$$\delta t_b' = \delta t_j + \delta t_p \tag{7}$$

Experimental Jitter

Shown in Figure 1 is a schematic of a jet emerging from a nozzle plate and breaking up into droplets. The break-up length L and its fluctuation δL are indicated. Also indicated in the figure, for two adjacent droplets, are position and time differences that are measured experimentally (between droplet centers indicated by red vertical dashed lines). The break-up length indicated in Figure 1 is the distance from the nozzle plate to the center of the droplet as it emerges from the jet.

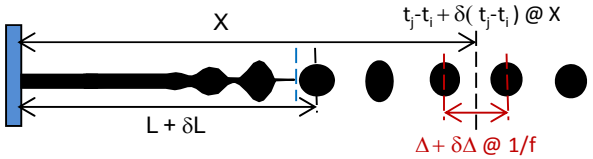

Figure 1. *Schematic of stimulated fluid jet emerging from a nozzle plate and associated droplet stream is shown. The indicated break-up length, position, droplet spacing, time differences, and their fluctuations are discussed in the text.*

The position x of a droplet in the stream is the sum of the breakup length L and the flight distance from break-up *(x-L)* in the direction along the jet axis. Hence, in terms of time and velocity the position is given by:

$$x = v_{jet}t_b + v_{drop}\left(t - t_b\right) \tag{8}$$

Taking the differential of Equation 8, using Equation 4, and using the fact that t is controlled by the strobe and δt is effectively zero we have:

$$\delta x = L\frac{\delta v_{jet}}{v_{jet}} + \left(v_{jet} - v_{drop}\right)\delta t_b + \frac{\delta v_{drop}}{v_{drop}}\left(x - L\right) \tag{9}$$

In the laser detection scheme, the position x is fixed by experiment and, therefore, δx is effectively zero, whereas δt is measured. One then finds that the quantity $-v_{drop}\delta t$ is equal to the right side of Equation 9. The experimentally measured quantity is the root-mean-square fluctuation, or standard deviation. Hence, in the laser detection scheme we find:

$$v_{drop}\sigma_t = \sqrt{\left[L\frac{\delta v_{jet}}{v_{jet}} + \left(v_{jet} - v_{drop}\right)\delta t_b + \frac{\delta v_{drop}}{v_{drop}}\left(x - L\right)\right]^2} \tag{10}$$

where σ_t is the measured standard deviation in arrival time (i.e., $\sigma_t = \sqrt{<\delta t^2>}$). Evaluation of the squared term in brackets requires some care. In particular, some fluctuations are likely correlated with one another, while other fluctuating quantities are statistically independent. In the former case, cross terms are not expected to vanish, whereas in the latter case, the cross terms can be expected to average to zero.

Experimental Jitter with Contributions from the Nozzle and Pinch-off Regions

As discussed earlier, the break-up time can be influenced by fluctuations in the nozzle bore and pinch-off regions. The effect of the fluctuations in the nozzle on the droplet velocity was described above (Equation 3). The effects of fluctuations at pinch-off on droplet velocity, however, have not been described in any detail. For now we simply consider two contributions to fluctuations in droplet velocity. Similar to the break-up time fluctuations of Equation 7, we write the drop velocity fluctuations as:

$$\delta v_{drop} = \delta v_j + \delta v_p\,, \tag{11}$$

where δv_j and δv_p are respective contributions from jet velocity fluctuations and fluctuations in the pinch-off region to fluctuations in droplet velocity.

We further assume that the drop velocity fluctuations δv_p caused by fluctuations in the pinch-off region are related to the break-up time fluctuations δt_p caused by fluctuations in that region. Including separate contributions from nozzle and pinch-off regions to the fluctuations in break-up time (*i.e.,* $\delta t = \delta t_j + \delta t_p$) and droplet velocity (*i.e,* Equation 11), Equation 10 becomes:

$$v_{drop}\sigma_t = \sqrt{\left[L\frac{\delta v_{jet}}{v_{jet}} + \left(v_{jet} - v_{drop}\right)\left(\delta t_j + \delta t_p\right) + \frac{\left(\delta v_j + \delta v_p\right)}{v_{drop}}\left(x - L\right)\right]^2} \tag{12}$$

While we expect $\delta v_j / v_{drop}$ ($\equiv J_j$) and $\delta v_p / v_{drop}$ ($\equiv J_p$) to be correlated, fluctuations introduced at pinch-off may be statistically independent from those occurring at the nozzle. In this case, δt_p is treated as statistically independent from all the other fluctuating quantities, except J_p (the fractional velocity jitter from pinch-off), which is presumably correlated with δt_p. Similarly, $\delta v_{jet} / v_{jet}$ ($\equiv J_{jet}$) is presumed to be correlated with δt_j (as well as with the radial perturbation fluctuation $\delta\xi_i$). Squaring Equation 12 and setting cross terms for statistically independent quantities to zero, we find:

$$(v_{drop}\sigma_t)^2 = a + b(x-L) + c(x-L)^2, \text{where}$$
$$a = \left[L^2 J_{jet}^2 + 2LJ_{jet}(v_{jet}-v_{drop})\delta t_j + (v_{jet}-v_{drop})^2(\delta t_j^2 + \delta t_p^2)\right]$$
$$b = \left[2LJ_j J_{jet} + 2(v_{jet}-v_{drop})(J_j \delta t_j + J_p \delta t_p)\right], \text{and}$$
$$c = \left(J_j^2 + J_p^2\right) \quad (13)$$

Here we use a, b, and c to denote respective constant, linear, and quadratic coefficients for the dependence of $(v_{drop}\sigma_t)^2$ on $(x\text{-}L)$.

Experimental Details

This work employed a test stand with a fixture to mount and translate an ink manifold and nozzle array assembly. In this test stand, three translation stages along orthogonal axes enable movement of the nozzle array along an optical axis normal to the plane containing the fluid jetted from the array (z), along the array axis (y), and along the jet axis (x). The y, x, and z axes are respectively for selecting the jet to be probed, the distance from the nozzle plate, and the focus.

A schematic of the drop detection apparatus is shown in Figure 2. The *y* translation stage is moved until a particular jet axis intersects the beam axis of a diode laser. As droplets travel downward through the stream they modulate the laser beam as they pass through it. A lens system images a portion of the curtain of jets onto a photodetector. The signal from the photodetector is input to a drop detection circuit that generates a positive pulse from the modulation of light intensity that occurs when a droplet passes through the laser beam. The output of the drop detection circuit is input to a computer controlled system that records drop arrival times, departure times and peak heights and computes statistics on specified sequences of droplets at specified locations along a jet.

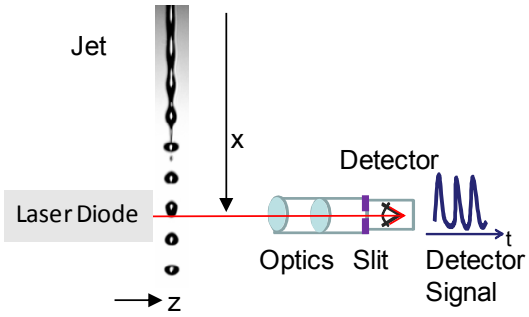

Figure. 2. *Schematic of the diode laser drop detection scheme. As drops travel downward through the stream, they intersect the laser beam modulating the intensity of light that reaches the detector through the sampling slit.*

The spatial magnification provided by the lens system is a factor of ten. A slit placed immediately in front of the detector has a width (y direction) of 150 µm and a height (x direction) of 25 µm. Hence, the region of the jet curtain that is imaged onto the detector is 15 µm x 2.5 mm. The width resolution is sufficient to resolve individual jets at 600 npi, and the height resolution is sufficient to resolve individual droplets (roughly 17 µm diameter fundamental droplets from 9.6 µm diameter nozzles). Although not shown in Figure 2, the apparatus also can be operated to capture images of the droplet stream. During imaging mode, a LED is strobed synchronously with drop generation and the drops are imaged using a CCD camera.

Results

In order to verify the models, a commercial black pigmented ink was jetted in our system at sufficient pressure to produce droplet velocities of roughly 20 m/s. A single nozzle was operated at the experimentally determined optimum frequency, where BOL (L) was minimized using constant power stimulation. The amplitude of the voltage pulse to the heater was then varied with a fixed pulse width in order to obtain a series of stimulation levels.

The BOL (L) and droplet velocity (v_{drop}) were determined stroboscopically at each stimulation level; L decreases with increasing stimulation while v_{drop} was essentially constant. Next, the drop statistics were obtained using the laser-photodetecteor drop detection system, including the arrival time variation for the droplets as a function of distance from the nozzle. Data were collected from just before jet break-up (~ 0.5 mm) to 2 mm beyond the nozzle plate. At each voltage level, the values of L and v_{drop} were used to determine the effective stimulation ξ_i from Equations 1 and 4, using the physical properties of the ink to calculate v_{jet} and the growth rate α. Additionally, the measured L and v_{drop} were used with the arrival time variance (σ_t) as a function of distance from break-off to determine the coefficients *a-c* of Equation 13. Figure 3 illustrates the data gathered at the highest stimulation and the quadratic fit obtained. In this exercise, the fit was constrained to truncate at L since there is no drop velocity variation prior to break-off.

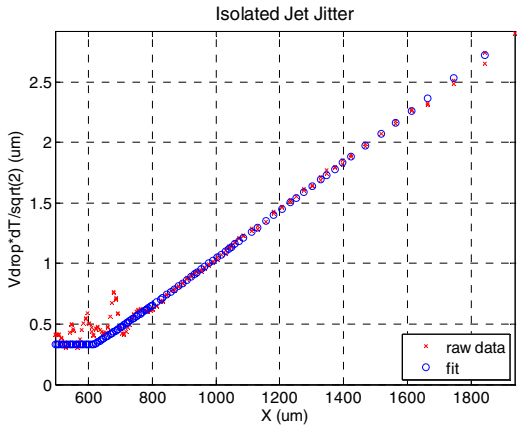

Figure. 3. *Data and model fit for a single isolated jet making droplets at the optimum frequency. Data is for the highest stimulation value used in the experiment.*

The coefficients from each stimulation level can be used to determine J_{jet}, J_p and J_j for each condition (the jet velocity jitter and the contributions to drop velocity jitter from pinch-off and the jet as discussed above). In order to calculate these quantities, two additional assumptions are required. The first is that the break-up time fluctuations from noise at pinch-off scale inversely with stimulation as described in Equation 14. Second, it is logical to constrain the pinch-off contribution to droplet velocity noise to scale with this break-up time fluctuation as described in Equation 15. In these equations g and h are constants.

$$\delta t_p = \frac{g}{\xi_i} \tag{14}$$

$$J_p = h\delta t_p \tag{15}$$

Adding the relationship between J_j and J_{jet} from Equation 3, one can then use the stimulation dependent coefficients to determine the noise parameters for the jet (*i.e.*, $\delta\xi_i$, J_{jet}, g and h). Results for the quadratic fitting coefficients are shown in Figs. 3a – 3c, with values normalized to the lowest stimulation value. As stimulation is increased, the overall arrival time variation decreases, as does each of the fitting coefficients.

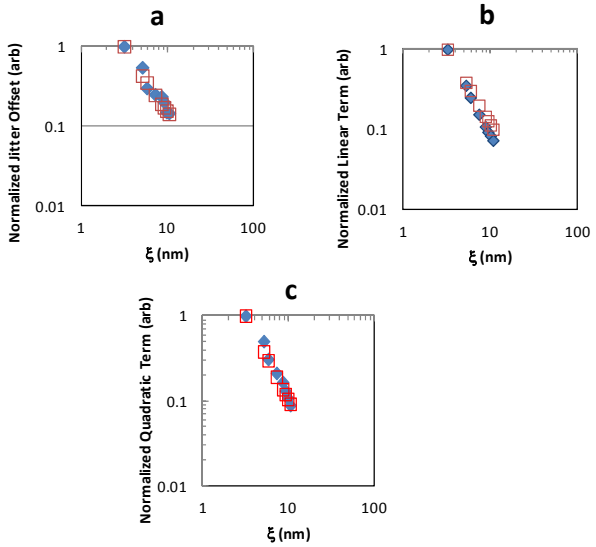

Figure 4. *Experimental values (diamonds) and modeled values (squares) for fitting parameters a, b, and c used to fit arrival time fluctuation data to Equation 13. The model data are generated by using a least squares method to determine the parameter set $\delta\xi_i$, J_{jet}, g and h that gives the best overall fit for all three parameters a, b, and c as a function of stimulation.*

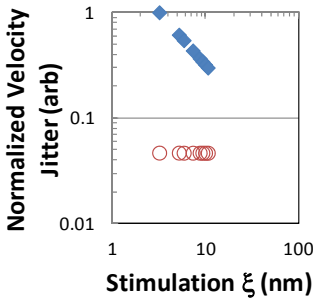

Figure 5. Contributions of J_p (diamonds) and J_j (circles) to the droplet velocity jitter as a function of stimulation. The data are normalized to the value of J_p at the lowest stimulation.

Based on the fitted noise parameters for the jet the relative contributions of fluctuations in the nozzle bore and at pinch off are determined as a function of stimulation (Figure 5). As shown in Figure 5, the contribution of fluctuations in the nozzle bore is relatively constant as a function of stimulation. The contribution from fluctuations at pinch-off dominate at low stimulation levels and become somewhat less dominant as stimulation is increased. The original premise that fluctuations in fluid properties in pinch-off region could have significant impact on the droplet velocity is supported by these results. As mentioned earlier, the fluid volume that couples the emerging droplet to the jet becomes vanishingly small in the region of pinch-off. In retrospect, it is not surprising that there is a significant contribution from the portion of the jet that is least stable.

Conclusions

Here we have described our analysis on a single jet at a fixed stimulation frequency and shown that the contributions to jitter in the pinch-off region dominate the overall droplet velocity jitter. Additional experiments have been conducted in our labs to tease out the relative effects of other aspects of droplet generation including frequency, fluid properties as well as stimulating multiple jets in an array. The mathematical and experimental treatment discussed here has been valuable in understanding the noise in a continuous drop generation system and enabling the design for robustness required for a commercial system.

References

[1] E. P. Furlani, "Temporal Instability of Viscous Liquid Microjets with Spatially Varying Surface Tension," J. Phys. A: Math. Gen., 38, 263–276 (2005).

[2] Stanley Middleman. Modeling Axisymmetric Flows: Dynamics of Films, Jets, and Drops (Academic, New York, 1995), pp. 102-112.

[3] V.V. Krotov and A.I. Rusanov, Physicochemical Hydrodynamics of Capillary Systems, (ICP, London, UK, 1999) pg. 271.

Author Biography

Jeremy M. Grace received his B.S. in Physics from MIT and his M.S. and Ph.D. in physics from the University of Illinois at Urbana-Champaign. After post-doctoral appointments at IBM and the Argonne National Laboratory, he worked Eastman Kodak Company in Rochester, New York. At Kodak, he worked in the areas of droplet generation in continuous fluid jets, plasma processing of materials, thin-film deposition processes, and plasma modification of polymer surfaces. He is now working in the field of thin film optical filters at Semrock, Inc, A Unit of IDEX Corporation.

Carolyn Ellinger received the B.S. degree in chemical engineering from the State University of NY at Buffalo and an M.S. degree in chemical engineering from the University of Rochester. She joined Eastman Kodak Company, Rochester, NY, in 1997, holding technical positions in AgX imaging systems, flexible displays, nanotechnology semiconductor devices, MEMS-based inkjet printhead design and fabrication, and inkjet printhead characterization. She is currently in the Kodak Technology Center.

Giuseppe Farruggia joined Eastman Kodak Company, Rochester, NY, in 1981 working on experimental thin-film deposition processes for electronics, including organic light emitting diodes (OLEDs). He is currently in the Kodak Technology Center working on printing devices and microfluidic device characterization.

Yonglin Xie received a B.S. and a M.S. degree in physics from Peking University. He received a Ph.D. degree in physics from Boston University, and an executive MBA degree from the Simon School of Business at the University of Rochester. Prior to joining Kodak in 2005, he held positions at Peking University, Xerox Corporation, and Trident – An ITW Company. He is currently in the Kodak Technology Center working on printing devices, microfluidics, and MEMS design and fabrication.